Anatomical insights into the proximal aponeurosis of the long head of the biceps femoris

Carmela Julia Mantecón-Tagarro,[1,2,3] Eri Nanizawa,[3] Munekazu Naito,[3,4] Shun Otsuka,[3,4] Huub Maas,[2] Yasuo Kawakami[1,3,4]

[1]Faculty of Sport Sciences, Waseda University, Saitama, Japan
[2]Department of Human Movement Sciences, Faculty of Behavioural and Movement Sciences, and Amsterdam Movement Sciences, Vrije Universiteit Amsterdam, The Netherlands
[3]Department of Anatomy, Aichi Medical University, Aichi, Japan
[4]Human Performance Laboratory, Comprehensive Research Organization, Waseda University, Tokyo, Japan

ABSTRACT

The biceps femoris long head (BFlh) is prone to strain injuries, but its reasons remain unclear. This study analyzed the BFlh proximal intramuscular aponeurosis in donor samples (n=4) through morphometric, microscopic, and histological methods. Cross-sections were taken every 5% of the muscle belly to differentiate connective, adipose, and muscle tissues. The aponeurosis extended from the muscle surface, becoming intramuscular from 40-70% of the muscle belly, and ended distally. Quantitative analysis revealed significant reductions of size in both the cross-sectional area (CSA) and width of the aponeurosis at 50% of muscle length, with CSA ranging from 4.9 mm² to 13.4 mm² and widths from 6.8 mm to 12.4 mm across subjects. Dense connective tissue bundles were separated by adipose or loose connective tissues. The aponeurosis shape varied along the muscle, with T- and hook-shaped configurations, and small branches were observed distally. These findings reveal the BFlh proximal aponeurosis as a complex structure, potentially influencing its injury susceptibility.

Key words: hamstrings; architecture; aponeurosis.

Correspondence: Yasuo Kawakami, Faculty of Sport Sciences, Waseda University, 2 Chome-579-15 Mikajima, 359-1192, Tokorozawa, Saitama, Japan. E-mail: ykawa@waseda.jp

Contributions: CJMT, conception and design of research plan, dissection and histology, data interpretation, manuscript drafting; EN, SO, conception and design of research plan, dissection, and histology support; MN, conception and design of research plan; HM, supervision and support in data analysis/interpretation and drafting the manuscript, critical revision and approval of manuscript; YK, conception and design of research plan, supervision and support in data analysis/interpretation and drafting the manuscript, critical revision and approval of manuscript.

Conflict of interest: the authors declare no competing interest.

Ethics approval: this study protocol was approved by the Ethical Committee of Aichi Medical University (approval number [2019-012]) in accordance with the Declaration of Helsinki. Signed donors' consent was obtained.

Availability of data and materials: the datasets used and/or analyzed during the current study are available upon reasonable request from the corresponding author.

Funding: this study was supported by JSPS Kakenhi (Fostering Joint International Research B, 21KK0175), JST SPRING (Grant Number JPMJSP2128) and JSPS Kakenhi (22K17722). The funder had no role in the design, data collection, data analysis, and reporting of this study.

Introduction

The biceps femoris long head (BFlh) muscle is in the posterior thigh, responsible for hip extension and knee flexion. It originates from the ischial tuberosity and inserts onto the head of the fibula. BFlh is more prone to injuries than its synergistic hamstring muscles, but the reasons remain unclear.[1,2] Its architectural complexity is thought to contribute to this susceptibility.[3-6] Recent studies have focused on BFlh's intricate structure, particularly the proximally located intramuscular aponeurosis (PIApo) as the hot spot of strain injury. Aponeurosis is a broad, sheet-like elastic connective tissue that extends along the muscle length, on the surface of muscle belly or inside of it and serves as an interface and a mechanical damper between the tendon and muscle fibers for fascicle attachment.[7,8] Understanding the PIApo three-dimensional (3D) architecture may provide insights into BFlh mechanical behavior during exercise and its injury prevention. However, knowledge of PIApo of BFlh is limited. Among approaches to PIApo of BFlh, *in vivo* studies used 2D ultrasonography to visualize its longitudinal and transverse shapes,[8,9] but this single-plane view is insufficient to capture complex structures of PIApo which is three-dimensional in nature. The 3D ultrasonography[10,11] can be a feasible alternative, but it cannot resolve structural details at the microscopic level that should provide insights into the strain injury mechanisms around PIApo. Direct observation of human donor specimens will allow minute examination of PIApo structure that can be combined with histological separation of the components that differ mechanical interactions with muscle fibers. To our knowledge, no study has ever detailed the PIApo of BFlh at the microscopic level. This study aims to offer a detailed structural feature of BFlh's PIApo, aiming to provide an insight into the injury mechanism around this "hot spot." Here we show that BFlh PIApo is not a simple sheet-like structure but rather has forms much more complex than ever imagined.

Materials and Methods

Ethics approval

This study protocol was approved by the ethical committee of Aichi Medical University (approval number [2019-012]) in accordance with the Declaration of Helsinki. Signed donors' consent was obtained.

Morphometric data collection

Prior muscle dissection, morphometric data, including thigh length (from the greater trochanter to the lateral epicondyle) and muscle-tendon unit length (from the ischial tuberosity to the fibular head attachment of BFlh), were collected from the donors (2 males:2 females, 84.5±6.4 years (means ± SD). The BFlh muscle belly was divided into blocks by cross-sectional cuts at 5% intervals (0% = proximal, 100% = distal). To prevent deformation, muscle belly samples were frozen in liquid nitrogen after being split at 50% of their length. A custom-made holder with two aluminum foil layers was used to avoid direct nitrogen contact. Samples were immersed for 70-100 s and stabilized using a wooden plank. Both sides of each block's cross-section were photographed with a high-resolution camera (EOS M50, Canon). This resulted in mirror images of each surface at 5% intervals, with aponeurosis visually identified in each image.

Microscopic analysis

A stereo macroscope (Nobita T [YS05T, Micronet], Japan) with a digital image system (Power Zoom Lens Kit E PZ 16-50 mm F3.5-5.6, ILEX-QX1, Sony, Japan), connected to an image storage app (Imaging Edge app) and cold light illumination (Cold light illuminator SCHOTT KL 1500 LCD, Japan) was used. Dense connective tissue of the aponeurosis was differentiated from loose connective and adipose tissue based on appearance and resistance to external loads using two micro-forceps under the microscope.

Histological analysis

For muscle blocks with unclear aponeurosis structure identification or location histological analysis was conducted using Masson's trichrome staining on one BFlh (right or left leg) of subjects 1, 2, and 3 (randomly selected). Additionally, as the PIApo location was within 40% to 70% of the BFlh muscle belly length, histological analysis was performed at 50% and 60% for all subjects to assess inter-individual variability. For subject 4, comparisons were made between both legs to assess intra-individual variability. One cross-section surface from each selected block was chosen. Samples were fixed in 20% formalin for one week, followed by paraffin infiltration (35 h), embedding, and slicing with a microtome (ESM 100-L Precision Sledge Microtome, AGD Biomedical, Japan) to prepare a slice with a thickness of 10.5-11 µm.[12] Subsequently, Masson's trichrome staining was applied,[13] highlighting collagen fibers and distinguishing dense connective tissue (organized bundles), loose connective tissue (disorganized), adipose tissue, and muscle fibers. After staining, keratin and muscle fibers appeared red, collagen blue and bone green, nuclei black, and adipose tissue white (Figure 1). Images of stained sections were taken using a microscope camera (all-in-one fluorescence microscope, BZ-X700, Keyence, Japan), with image stitching applied to create high-resolution images of the full cross-section at high magnification.

Cross-sectional area and width analysis

The cross-sectional area (CSA) and width of both the aponeurosis and muscle were quantitatively analyzed using a custom-made MATLAB (MathWorks. (n.d.) Natick, MA, USA, MATLAB (R2024a) [Software]) script. The width of the aponeurosis was defined as the largest distance between its superficial and deep surfaces in the cross-sectional plane, regardless of the shape of the aponeurosis. This analysis was performed on the high-resolution

Table 1. Sex, age, thigh and muscle-tendon unit length of right and left leg for each subject.

	Sex	Age	Right thigh length (cm)	Right BFlh MTU length (cm)	Left thigh length (cm)	Left BFlh MTU length (cm)
Subject 1	Male	85	33.0	35.4	34.3	38.4
Subject 2	Female	85	36.5	38.1	37.6	38.3
Subject 3	Female	93	34.1	38.0	33.5	37.1
Subject 4	Male	75	34.0	36.4	34.1	35.8

MTU, muscle-tendon unit.

images from Masson's trichrome stained samples at 50% and 60% of the BFlh muscle belly length. Additionally, paired t-test was performed to compare differences between 50% and 60% of PIApo CSA and width as well as muscle CSA.

Results

Morphological measurements showed similar results between right and left legs across all samples with no significant differences (Table 1). The proximal aponeurosis extended from the muscle's external borders proximally to deeper within the muscle distally. An aponeurotic sheet extended from the proximal tendon end along the medial side of the muscle's exterior, and another sheet developed internally toward the ventral side, forming the PIApo. PIApo appeared from approximately 40±5% to 70±5% of the muscle belly length, with shape changes at 50% of the length (Figure 1). In some cases, it was in contact with the muscle border (Figure 1A), while in others, it was closer to the center (Figure 1C). Similar shape was observed in both legs of subject four (Figure 1 D,E).

PIApo and muscle morphological measurements are shown in Table 2. At 50% of the muscle length, the PIApo CSA ranged from

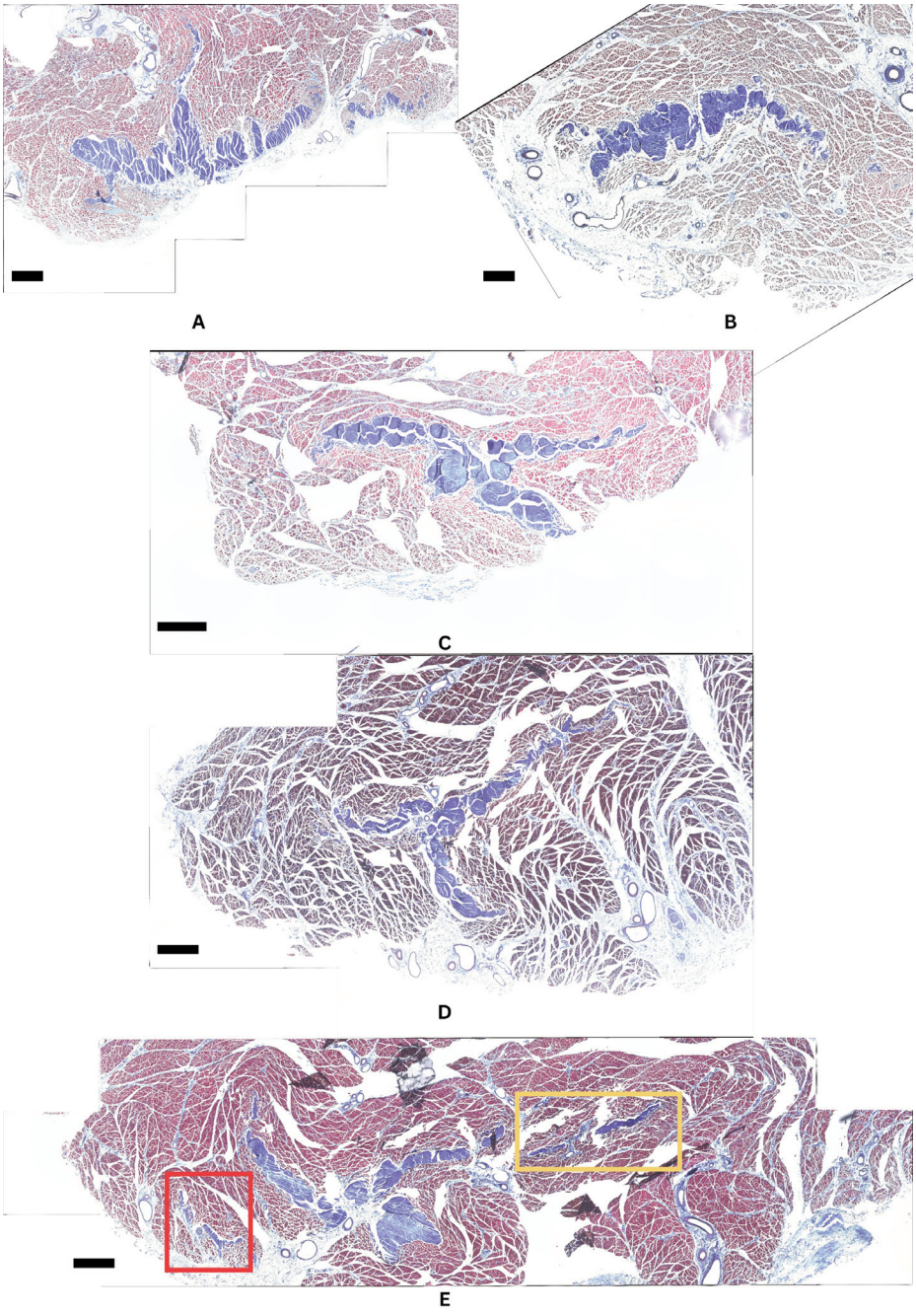

Figure 1. Different shapes of the intramuscular aponeurosis (stained blue) at 50% of BFlh muscle belly length. **A**) Subject 1 (left leg). **B**) Subject 2 (right leg). **C**) Subject 3 (right leg). **D**) Subject 4 left leg. **E**) Subject 4 right leg. Red and gold squared areas in panel E indicate clusters of aponeurosis-like dense connective tissue independent from the main intramuscular aponeurosis. Scale bars: 1000 µm.

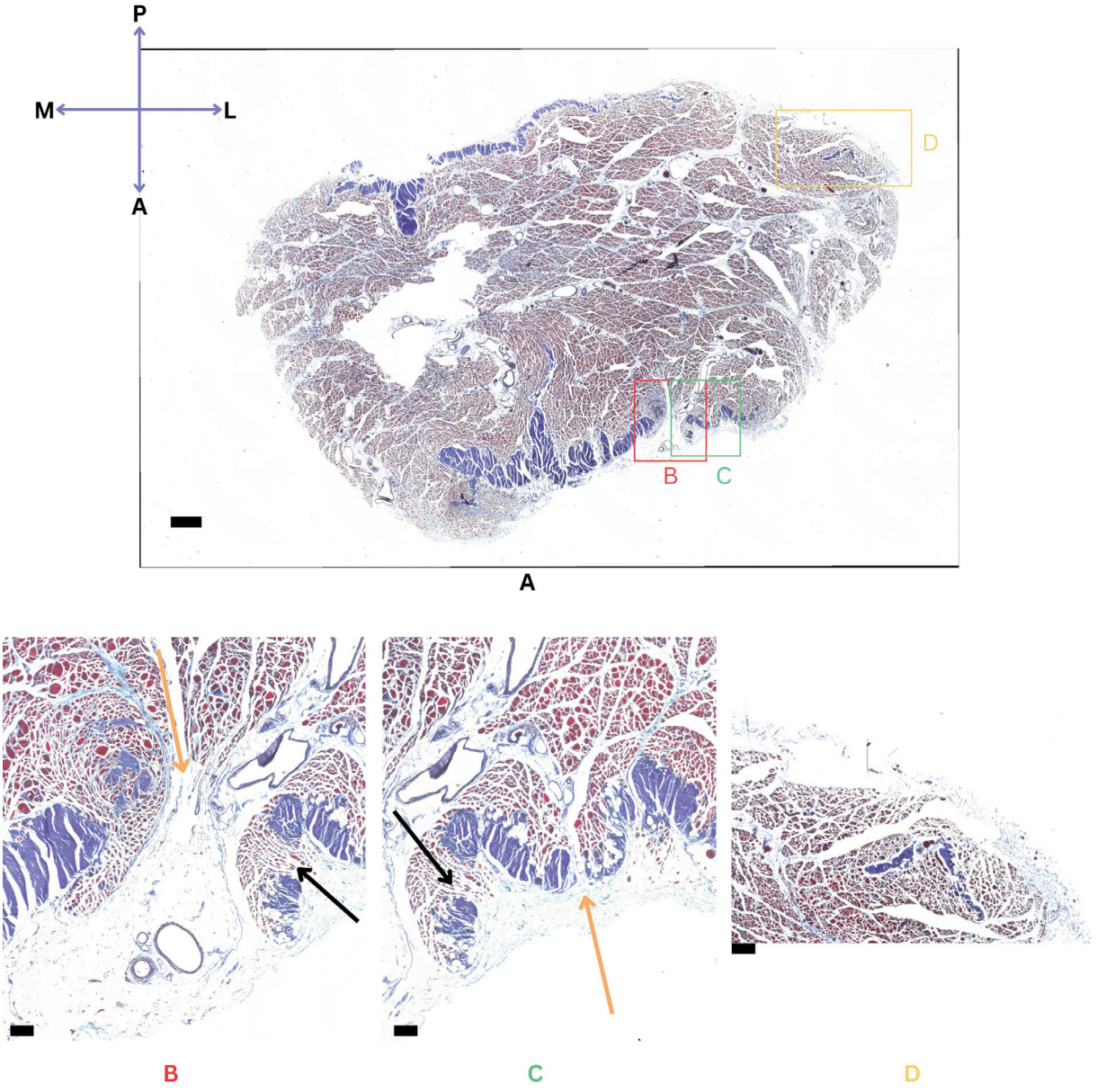

Figure 2. A) Full CSA image of one sample at 50% of BFlh muscle belly length after Masson's trichrome staining; keratin and muscle fibers in red, collagen in blue, and adipose tissue in white/transparent; CSA of subject 1 left leg; bottom, from left to right, 3 enlarged images of the CSA; scale bar: 1000 µm. **B**) Aponeurosis interrupted by adipose tissue. **C**) Aponeurosis interrupted by muscle fibers. **D**) Clusters of aponeurosis-like dense connective tissue independent from the main intramuscular aponeurosis. Black arrows in panels B and C indicate aponeurotic disruption by muscle tissue and orange arrows indicate aponeurotic disruption by adipose tissue; B,C,D) scale bars: 200 µm. All the images present the same orientation and alignment indicated by the cross arrows on the top left corner, with posterior area (P) on top, lateral area (L) to the right, medial area (M) to the left and anterior area (A) (closer to the humerus bone) on the bottom of the image.

Table 2. Aponeurosis CSA, width, length, and muscle CSA at 50% and 60% of muscle length.

	Leg	PIApo CSA 50% (mm^2)	PIApo Width 50% (mm)	Muscle CSA 50% (mm^2)	PIApo CSA 60% (mm^2)	PIApo Width 60% (mm)	Muscle CSA 60% (mm^2)
Subject 1	Left	13.4	12.4	177.2	4	4.7	202.6
Subject 2	Right	7.2	6.9	152.6	4.5	6.1	115.5
Subject 3	Right	4.9	6.9	90.9	1.6	2.9	70.6
Subject 4	Right	5.6	8.8	180.5	0.5	1.5	143.6
Subject 4	Left	5.2	7.8	195.5	1.5	1.9	142.9

PIApo, proximal intramuscular aponeurosis; CSA, cross-sectional area.

4.9 mm² to 13.4 mm² and width from 6.8 mm to 12.4 mm across five legs, while muscle CSA ranged from 90.9 mm² to 195.5 mm². At 60%, PIApo CSA and width showed notable reductions, with PIApo CSA ranged from 0.5 mm² to 4.5 mm² and width from 1.5 mm to 6.1 mm across five legs, while muscle CSA ranged from 70.6 mm² to 202.6 mm². Paired t-test showed significant differences between 50% and 60% in PIApo CSA (p=0.015) and PIApo width (p=0.016), but not significant for muscle CSA (p=0.145). Microscopic and histological analyses showed separation of the collagen bundles of the proximal aponeurosis by loose connective tissue, adipose tissue, and/or muscle fibers, interrupting the aponeurotic continuity across all subjects (Figure 2 B,C). The PIApo varies in size and shape along the muscle length. At 50% of the muscle length, one subject exhibited a T-shaped aponeurosis that transformed into a flat-like line at 60% (Figure 3 A,B). Another subject, a wider hook-shaped cross-section with adipose tissue separations at 50% narrowed at 60% (Figure 3 C,D), being sometimes flatter and sometimes more curved.

Lastly, small independent aponeurosis-like structures were identified within the muscle (*i.e.* not part of the main PIApo) in subject 1 (Figure 2D) and subject 4 right leg (Figure 1E). In total, three structures were found, with CSA of 0.4 mm² for all three structures, and widths of 1.8 mm for subject 1 and 1.7 (Figure 1E, red square) and 2.6 mm (Figure 1E, gold square) for subject 4.

Discussion

Results show the complexity of BFlh PIApo. The primary features identified include: i) a discontinuous structure composed of dense connective tissue bundles interrupted by adipose tissue, loose connective tissue, and muscle fibers; and ii) hook- or T-shapes. These structures extend from the muscle's external borders proximally to deeper within the muscle distally. Quantitative measurements confirmed substantial inter-individual differences in PIApo CSA, and width at 50% of the muscle belly. Additionally, the PIApo seems to not be homogeneous along the BFlh muscle length, changing in size and shape.

The observed infiltration of other tissues between the dense connective tissue bundles indicates that the PIApo is segmented as the plantar fascia.[13] This structural organization may allow greater transversal deformations[14] due to more freedom of movement on the lateral/transverse direction during contractions, helping the muscle adapt to varying mechanical demands. This pattern was

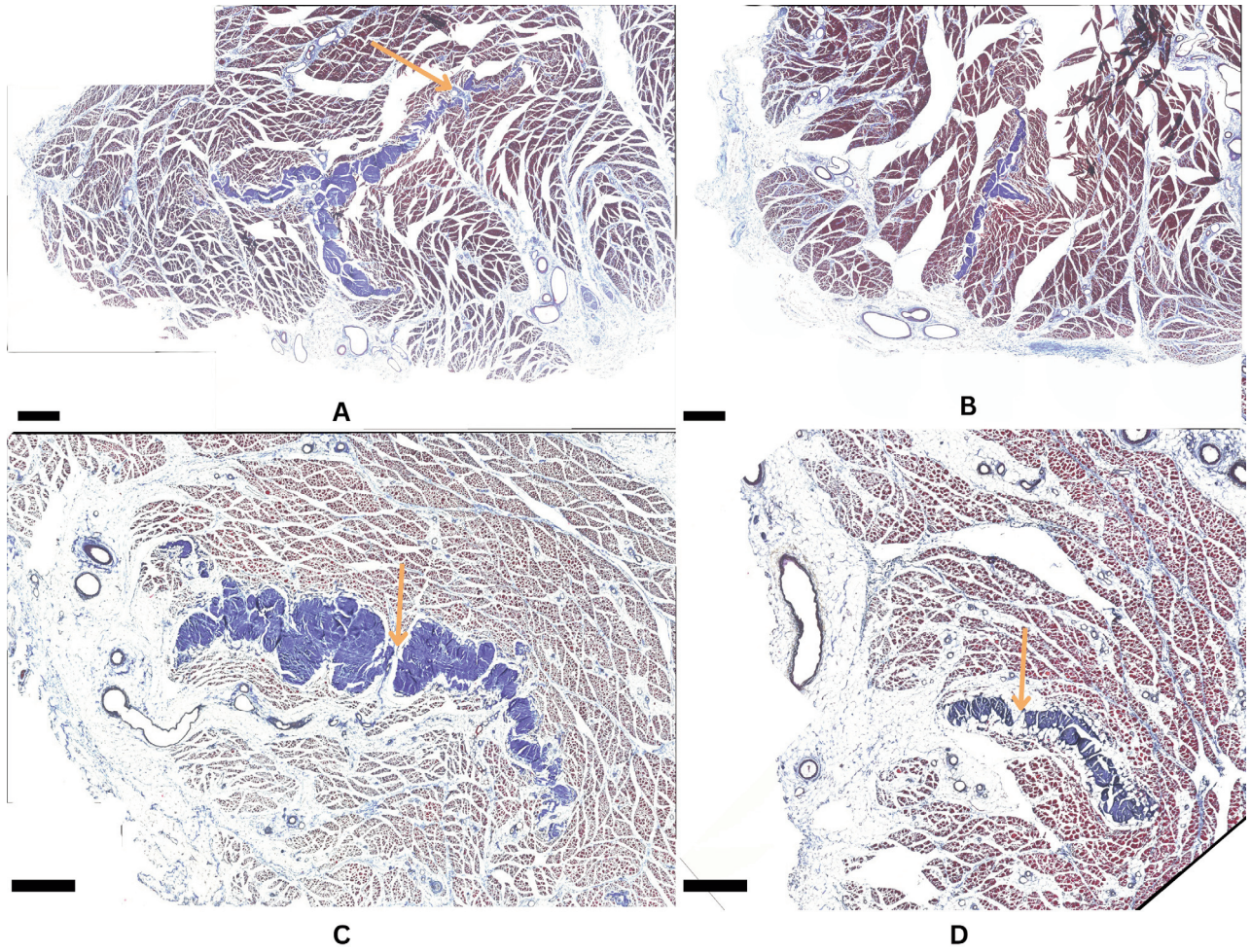

Figure 3. Different sizes and shapes of the aponeurosis (stained dark blue) in the CSA at 50% (left) and 60% (right) of the BFlh muscle belly length of subject 4 left leg (**A,B**) and subject 2 right leg (**C,D**). Different sizes and shapes of the aponeurosis (stained dark blue) in the CSA at 50% (left) and 60% (right) of the BFlh muscle belly length of subject 4 left leg (**A,B**) and subject 2 right leg (**C,D**). Scale bars: 1000 µm.

consistently observed across all subjects, suggesting a common anatomical characteristic and potential functional role.

The shape of the PIApo changed along the muscle length. At approximately 50% of the muscle length, the PIApo exhibited various shapes, such as T-shaped or hook-shaped, transforming into a flatter and narrower structure at around 60%. This visual observation was supported by statistical analysis, which showed significant reductions in both PIApo CSA and width between 50% and 60%, indicating a marked narrowing and thinning of the aponeurosis in the distal region. These findings suggest a region-specific change that may affect how mechanical stress is transmitted along the muscle. In particular, the thinner and narrower aponeurosis in the distal region might experience different stress concentrations during contraction, potentially influencing the alignment and loading patterns of the attached fascicles. Furthermore, inter-individual and intra-individual differences were observed. For inter-individual differences, morphology changes in PIApo at comparable locations may have mechanical implications. Previous studies have linked differences in the shape of the PIApo, specifically the width, to the risk of injury.[8,15,16] As previously stated, changes in aponeurosis size and shape could influence susceptibility to mechanical stress, with thinner aponeuroses potentially being less effective in distributing force, increasing the risk of injury during activities like high-speed running. However, there is no consensus about this,[8] and whether such a link exists for the features described in this study remains unknown. For intra-individual consistency, differences in aponeurosis shapes between the left and right legs of one subject were assessed and similar shapes were observed, as well as their width and CSA, suggesting consistency within individuals. Nevertheless, the observed inter-individual variability underscores the need for further investigation to explore how aponeurosis features influence muscle mechanics and injury risk.

Small independent aponeurosis-like structures within the muscle, which were not part of the main PIApo, suggesting a more complex intramuscular connective tissue network than previously understood. For instance, one of these structures, although small, was clearly distinguishable and embedded within the muscle tissue. The presence of such structures, even at this scale, may indicate a functional role in force transmission and redistribution within the muscle. Their position within the muscle suggests they could facilitate more effective transmission of muscle fiber-generated forces to the external tendon and skeleton by providing additional pathways for force distribution. Conversely, their small size and isolated nature might introduce localized disruptions or uneven force transmission, potentially affecting efficiency during contraction. Further investigation is needed to confirm whether these structures are indeed aponeurotic tissue and, if so, determine whether these structures enhance or hinder muscle performance.

This study improves our understanding of the BFlh PIApo's structural features, but some limitations should be noted. The use of embalmed human donors may not fully represent *in vivo* conditions, and further studies using *in vivo* techniques are needed to develop a gold-standard methodology and provide additional insights into the dynamic behavior of PIApo during muscle contraction. The small sample size limits the generalizability. Although factors such as age, sex and physical fitness have been linked to aponeurosis stiffness and injury susceptibility in previous research, these variables could not be meaningfully evaluated in the present study. Further studies with larger sample sizes and diverse populations are necessary. The resistance to external loads was not quantified although differences between tissue types were substantial. Finally, even though the adipose tissue infiltration was qualitative reported, due to inconsistencies in tissue quality and segmentation precision, adipose tissue infiltration could not be reliably quantified across all samples.

In conclusion, the PIApo of BFlh exhibits a discontinuous connective tissue sheet, including small aponeurosis-like structures within the muscle. These structures vary in size, shape, and position between subjects. While intra-individual consistency was observed, inter-individual variability, particularly in aponeurosis width and CSA, underscores its potential relevance to injury susceptibility. Independent structures suggest a more complex connective tissue network, warranting further investigation into their biomechanical implications. Future research should focus on the mechanical consequences of these features.

Acknowledgements

Our deepest gratitude and recognition to those who contribute to this study by donating their bodies to science and their families, making this research possible. Thanks to Aichi Medical University for lending us its facilities and resources to carry out this study.

References

1. Bourne MN, Opar DA, Williams MD, Shield AJ. Eccentric knee flexor strength and risk of hamstring injuries in rugby union. Am J Sports Med 2015;43:2663-70.
2. Battermann N, Appell H-J, Dargel J, Koebke J. An anatomical study of the proximal hamstring muscle complex to elucidate muscle strains in this region. Int J Sports Med 2010;32:211-5.
3. Maganaris CN, Kawakami Y, Fukunaga T. Changes in aponeurotic dimensions upon muscle shortening: in vivo observations in man. J Anat 2001;199:449-56.
4. Schache AG, Ackland DC, Fok L, Koulouris G, Pandy MG. Three-dimensional geometry of the human biceps femoris long head measured in vivo using magnetic resonance imaging. Clin Biomech 2013;28:278-84.
5. Kellis E. Biceps femoris and semitendinosus tendon/aponeurosis strain during passive and active (isometric) conditions. J Electromyogr Kinesiol 2016;26:111-9.
6. Kellis E. Intra- and inter-muscular variations in hamstring architecture and mechanics and their implications for injury: a narrative review. Sports Med 2018;48:2271-83.
7. Azizi E, Roberts TJ. Biaxial strain and variable stiffness in aponeuroses. J Physiol 2009;587:4309-18.
8. Evangelidis PE, Massey GJ, Pain MTG, Folland JP. Biceps femoris aponeurosis size. Med Sci Sports Exerc 2015;47:1383-9.
9. Freitas SR, Abrantes F, Santos F, Mascarenhas V, Oliveira R, Firmino T, et al. Is biceps femoris aponeurosis size an independent risk factor for strain injury? Int J Sports Med 2020;41:552-7.
10. Haberfehlner H, Maas H, Harlaar J, Becher JG, Buizer AI, Jaspers RT. Freehand three-dimensional ultrasound to assess semitendinosus muscle morphology. J Anat 2016;229:591-9.
11. Weide G, van der Zwaard S, Huijing PA, Jaspers RT, Harlaar J. 3D ultrasound imaging: fast and cost-effective morphometry of musculoskeletal tissue. J Vis Exp 2017;129:55943.
12. Farfán E, Rojas S, Olivé-Vilás R, Rodríguez-Baeza A. Morphological study on the origin of the semitendinosus muscle in the long head of biceps femoris. Scand J Med Sci Sports 2021;31:2282-90.
13. Stecco C, Corradin M, Macchi V, Morra A, Porzionato A, Biz C, De Caro R. Plantar fascia anatomy and its relationship with Achilles tendon and paratenon. J Anat 2013;223:665-76.
14. Shan X, Otsuka S, Yakura T, Naito M, Nakano T, Kawakami Y. Morphological and mechanical properties of the human triceps

surae aponeuroses taken from elderly cadavers: implications for muscle-tendon interactions. PLoS One 2019;14:e0211485.
15. Fiorentino NM, Epstein FH, Blemker SS. Activation and aponeurosis morphology affect in vivo muscle tissue strains near the myotendinous junction. J Biomech 2012;45:647-52.
16. Rehorn MR, Blemker SS. The effects of aponeurosis geometry on strain injury susceptibility explored with a 3D muscle model. J Biomech 2010;43:2574-81.

Received: 25 November 2024. Accepted: 17 April 2025.

European Journal of Histochemistry 2025; 69:4165
doi:10.4081/ejh.2025.4165